J. Cell. Mol. Med. Vol 12, No 3, 2008 pp. 899-913

Vasomotion dynamics following calcium spiking depend on both cell signalling and limited constriction velocity in rat mesenteric small arteries

Ed VanBavel *, Esther T. van der Meulen, Jos A. E. Spaan

Academic Medical Center, University of Amsterdam, Department of Medical Physics, Amsterdam, The Netherlands

Received: May 24, 2007; Accepted: October 9, 2007

Abstract

Vascular smooth muscle cell contraction depends on intracellular calcium. However, calcium-contraction coupling involves a complex array of intracellular processes. Quantitating the dynamical relation between calcium perturbations and resulting changes in tone may help identifying these processes. We hypothesized that in small arteries accurate quantitation can be achieved during rhythmic vasomotion, and questioned whether these dynamics depend on intracellular signalling or physical vasoconstriction. We studied calcium-constriction dynamics in cannulated and pressurized rat mesenteric small arteries (~300 μm in diameter). Combined application of tetra-ethyl ammonium (TEA) and BayK8644 induced rhythmicity, consisting of regular and irregular calcium spiking and superposition of spikes. Calcium spikes induced delayed vasomotion cycles. Their dynamic relation could be fitted by a linear second-order model. The dirac impulse response of this model had an amplitude that was strongly reduced with increasing perfusion pressure between 17 and 98 mmHg, while time to peak and relaxation time were the largest at an intermediate pressure (57 mmHg: respectively 0.9 and 2.3 sec). To address to what extent these dynamics reside in intracellular signalling or vasoconstriction, we applied rhythmic increases in pressure counteracting the vasoconstriction. This revealed that calcium-activation coupling became faster when vasoconstriction was counteracted. During such compensation, a calcium impulse response remained that lasted 0.5 sec to peak activation, followed by a 1.0 sec relaxation time, attributable to signalling dynamics. In conclusion, this study demonstrates the feasibility of quantitating calcium-activation dynamics in vasomoting small arteries. These dynamics relate to both intracellular signalling and actual vasoconstriction. Performing such analyses during pharmacological intervention and in genetic models provides a tool for unravelling calcium-contraction coupling in small arteries.

Keywords: vascular smooth muscle • calcium • vasoconstriction • dynamics • pressure

Introduction

The constriction of blood vessels depends on the intracellular calcium concentration of the vascular smooth muscle cells (SMC). Yet, their relation is affected by many conditions, including the tissue, the presence of pathological conditions, the nature of the activating stimulus and the duration of its presence. Activation of G-protein-coupled receptors increases calcium sensitivity, while several vasodilators reduce sensitivity [1]. Potassium-induced depolarization is frequently used as standard when determining calcium

*Correspondence to: Dr. E VANBAVEL,
Academic Medical Center, PO Box 22700,
1100 DE Amsterdam, The Netherlands.
Tel.: +31-20-56 65 20 3
Fax: +31-20-69 17 23 3
E-mail: e.vanbavel@amc.uva.nl

doi: 10.1111/j.1582-4934.2007.00142.x

sensitivity, although recent work has indicated that also potassium may induce sensitization [2]. We found in rat mesenteric small arteries that also myogenic activation by pressure is associated with an increased calcium sensitivity [3]. Vasodilator therapy in hypertension and other cardiovascular disorders may include reduction of calcium sensitivity, by for example, inhibitors of rho kinase [4–6] and phosphodiesterase [7, 8], in addition to classic calcium-lowering drugs, such as the L-type calcium channel blockers. However, further evaluation of the potentials for reducing calcium sensitivity in pharmacotherapy would profit from a better understanding of the calcium-contraction coupling in microvascular smooth muscle.

Several strategies have been used to identify the events linking a rise in calcium and the subsequent vasoconstriction. These strategies include the use of blockers and the determination of concentration or activity of intracellular targets. However, such experiments are typically based on steady states only. Further information may come from the dynamic relation between sudden changes in calcium and the following vasoconstriction. Thus, studying this relation under a variety of conditions may allow identifying steps in the activation and desensitization processes that are critical determinants of sensitivity and thereby form possible targets for vasodilator therapy in cardiovascular pathologies. However, this dynamic relation has not been studied much in SMC, let alone in intact vascular segments and in the microvessels that determine peripheral resistance.

The purpose of this study is to analyze dynamic calcium-constriction relations in pressurized small arteries. In particular, we hypothesized that rhythmic vasomotion may provide a useful base for accurate quantitation of these relations. Vasomotion is observed in many small blood vessels *in vivo* [9]. In previous *in vitro* studies on cannulated or wire-mounted small arteries, we [10] and others [11] observed similar behaviour, either spontaneously or after application of a wide range of vasoactive agents. Vasoconstriction lags the calcium oscillations [12], but it is not clear whether this lag represents intracellular signalling or the limited constriction velocity of the SMC. In order to discriminate between these possibilities, we counteracted the rhythmic constrictions by simultaneously raising the pressure, using an automated feedback system. This way, isometric loading of the cannulated vessels is approximated and any remaining lag would be attributable to cell signalling. We additionally hypothesized that this lag is substantial, providing a rationale for studying such dynamics following pharmacological or genetic manipulation of signalling pathways in future work. As a first step, the current work shows that the calcium-vasoconstriction relation of rat mesenteric small arteries for the chosen conditions follows linear second-order dynamics, related to both signalling and actual vasoconstriction.

Methods

Cannulation

The methods used for the isolation and cannulation of the small mesenteric arteries have been described in detail previously [3]. In short, male Wistar rats were anaesthetized with pentobarbital (0.06 mg/g bodyweight) by intraperitoneal injection. After thoracotomy, the heart was removed for other purposes. The intestinal tract was removed, and small mesenteric arteries, inner diameter ranging between 272 and 378 μm (mean 331 μm) when at 98 mmHg and maximally dilated, were isolated, cannulated at both ends, using glass micro-cannulas, and sutured with 17 μm nylon filaments. After cannulation, vessels were pressurized to 98 mmHg and stretched until they appeared straight. Vessels were pressurized through both cannulas, using a Fairchild voltage-pressure converter. A pressure gradient between both pipettes of 1 mmHg was applied, in order to provide a small flow in the vessel. This sub-physiological flow did not cause flow-induced dilation or constriction. Vessels were immersed in physiological saline solution (PSS; composition (mmol/l): NaCl 119, KCl 4.7, KH_2PO_4 1.18, $MgSO_4$ 1.17, $NaHCO_3$ 25, $CaCl_2$ 1.6, ethylenediaminetetraacetic acid (EDTA) 0.026, glucose 5.5, Hepes 10, solution equilibrated with 19 % O_2, 76 % N_2, and 5 % CO_2, pH 7.35±0.05). The intraluminal fluid contained PSS supplemented with 0.5 % bovine serum albumin.

Diameter measurement

The state of constriction of the vessels was determined using a previously described volumetric fluorescence technique [13]. In short, the lumen of the vessel contained Texas Red-dextran, which was excitated at 560 nm. The total amount of emission light (>610 nm) was determined using a photomultiplier tube. A constricting vessel would push the dye back into the cannulas and out of the field of illumination, thereby reducing the fluorescence light. Since

the length of the illuminated part of the vessel as well as the dye concentration was kept constant, the fluorescence signal is proportional to the luminal cross-sectional area (CSA) of the vessel. Luminal diameter was determined from CSA, assuming that the vessel circumference is circular. Calibration of the diameter obtained in this fashion against eyepiece micrometer measurements was performed during application of a calcium-free solution, simultaneously with determination of the minimal Fura-2 fluorescence ratio (see below). Diameters were normalized to d_0, the diameter at 98 mmHg and full dilation. d_0 was determined during application of the calcium-free solution.

Measurement of the intracellular calcium concentration

50 µg fura-2 AM was dissolved in 50 µl dimethylsulphoxide containing 2 % pluronic and suspended in 5 ml PSS. The cannulated vessel was superfused with this loading solution for 1 hr at approximately 30°C, followed by a washout period of 30 min at 37°C. Excitation was achieved by common fluorescence microscopy using a 75W Xenon light source and a filter wheel rotating at around 40 Hz and containing 340 and 380 nm interference filters for the Fura-2 measurements, as well as a 560 nm filter for the determination of the diameter using Texas Red. A secondary dichroic mirror separated emission light from these two dyes. The calcium light was subsequently filtered at 515 nm, and measured by a photomultiplier tube. Appropriate sample-and-hold and filtering circuitry was used for both the fura-2 and Texas Red signals, and these signals were sampled at 50 Hz. Possible cross-talk between the fura and Texas Red fluorescence signals was below detection limits. Care was taken to limit the amount of exposure time to the fluorescence light.

At the end of each experiment maximal and minimal values for the 340/380 ratio were determined in the presence of 2 µmol/l ionomycin, 20 mmol/l NaCl, 150 mmol/l KCl, 10 mmol/l MOPS (pH = 7.3) and respectively 10 mmol/l $CaCl_2$ or 10 mmol/l EGTA. Finally, the fluorescence levels after quenching with 20 mmol/L $MnCl_2$ were determined. We did not attempt to quantitatively estimate the intracellular calcium concentration from the fura-2 light, due to uncertainties in the intracellular dissociation constant for fura-2. Rather, the following normalized ratio (R_n) was used as an index of the calcium concentration:

$$R_n = (R - R_{min}) / (R_{max} - R_{min}) \quad (1)$$

where R denotes the 340/380 ratio, corrected for fluorescence levels after quenching, and R_{max} and R_{min} the maximal and minimal values for this ratio. R_{max} and R_{min} were typically 1.2 and 0.2, while quenching reduced fluorescence light at both wavelengths to approximately 30% of the original levels.

Application of non-isobaric loading

In part of the experiments, we applied non-isobaric loading of the cannulated vessels in order to discriminate between the dynamics of intracellular signalling and actual smooth muscle cell shortening. Such mechanical loading consisted of partially preventing actual vasoconstriction by feedback adjustment of the pressure, based on the difference between the actual luminal CSA and a reference value. Proportional feedback was applied according to the algorithm

$$P(t) = P_i + k \cdot (CSA_i - CSA\ (t)) \quad (2)$$

with P the pressure, k the feedback gain and P_i and CSA_i the pressure and CSA at the start of the feedback algorithm, which serve as the reference point. Thus, depending on k, activation was reflected by only diameter reduction (k = 0) or by simultaneous diameter reduction and pressure elevation (k > 0). Pure isometric loading during rhythmic activity would require extremely high values for k, leading to instabilities, and this was avoided. The frequency response of the feedback circuit was limited by the voltage-pressure converter and was flat up to 5 Hz, which was sufficient to counteract the vasomotion cycles. Off-line, CSA values were converted to diameters.

Protocol

Vasomotion was induced by 1 µM of the L-type voltage-operated calcium channel opener BayK8644 in combination with 1 mM of the calcium-dependent potassium channel blocker tetra-ethyl ammonium (TEA). This combination was applied at 17 mmHg, and the vessel was maintained at this pressure for 15 min, followed by 15 min pressurization to 57, 98 and again 17 mmHg.

In a subset of the experiments, non-isobaric feedback was applied as indicated above. For each gain, the feedback algorithm was applied for only a few vasomotion cycles, interspersed by periods of isobaric vasomotion. This was done to prevent substantial drift of the level of contractile activity.

Chemicals

All vasoactive agents were applied by changing the superfusion solution. Noradrenaline, tetra ethyl ammonium chloride and ionomycin were obtained from Sigma. Bay K8644 was obtained from Bayer (Uerdingen, Germany). Fura-2

AM and Texas Red-dextran were from Molecular Probes (Eugene, Oregon).

Data analysis and statistics

Both the diameter and the calcium signals were sampled at 50 Hz. Recordings of these signals were divided in periods of around 30 sec, which were used as the basis for the fitting procedures. Periods without vasomotion were excluded from the analysis.

We attempted to fit two models to the calcium-constriction relation: model I is a first-order linear model based on the differential equation:

$$\tau \cdot \frac{dD_e}{dt} + D_e = a \cdot R_n + b \qquad (3)$$

with D_e the estimated normalized diameter as a function of time and R_n the calcium ratio signal. τ, a and b are the parameters to be determined. τ represents the time constant of this system, and a and b the gain and offset of the stationary relation.
model II is a second-order linear model, based on:

$$\alpha \cdot \frac{d^2D_e}{dt^2} + \beta \cdot \frac{dD_e}{dt} + D_e = a \cdot R_n + b \qquad (4)$$

with α and β, a and b the parameters to be determined. For both models, fitting was done in the time domain, using a fourth-fifth-order Runga-Kutta technique with a fixed integration interval of 0.02 sec. For each 30 sec vasomotion period, a set of parameters was determined that optimizes the goodness-of-fit, as expressed by the squared correlation coefficient:

$$r^2 = 1 - \frac{\Sigma(D_n - D_n)^2}{\Sigma(D_n - avgD_n)^2} \qquad (5)$$

where D_n is the observed normalized diameter and $avgD_n$ the average value. The summation is over all sample points in the 30 sec interval. The numerical integration of the differential equations requires choices for the initial conditions. In model I, the initial diameter is needed, while in model II also the initial constriction velocity at the start of the 30 sec period is required. These integration constants were determined from the first 100 msec of the measured diameter signal.

The above fitting procedures were performed on 486 periods of vasomotion in nine vessels at three pressures, resulting in 486 sets of parameters for each model. Subsequently, averages of the parameters were determined for each vessel and each pressure. In addition, the parameters obtained for model II were used to calculate the diameter response to a Dirac calcium impulse (*i.e.* an impulse with infinite amplitude, zero duration, and unity area under the curve), since this best characterizes the behaviour of the system in the time domain. Three descriptive parameters were then deduced from the impulse response (see also Fig. 5): the peak impulse response, the time of peak response, and the time of half-maximal relaxation. These descriptive parameters were also averaged for each vessel and pressure level.

Applied statistics were t-tests, ANOVAS or General Linear Models (GLM) with Bonferroni post-hoc tests where appropriate, and were applied using SPSS 11.5. Results are shown as mean±SEM, unless otherwise indicated. $P<0.05$ was considered statistically significant.

Results

Time-averaged calcium and constriction

Figure 1 plots the time-averaged diameter and calcium levels as functions of the distending pressure in the presence of 1 μM BayK 8644 and 1 mM TEA (filled symbols). These averages were determined over the period between 5 and 15 min after each pressure step. For reference, the available values under full dilation are also indicated (open symbols). The combined addition of the calcium agonist and potassium channel blocker resulted in an initial deep constriction (not shown) followed by a very shallow, though significant constriction. Increasing the pressure induced a significant distension of the vessel, while myogenic responses were absent. At 17 mmHg, the time-averaged calcium signal was not significantly higher in the presence as compared to the absence of both drugs (Fig. 1B). Increasing the pressure in the presence of TEA and BayK 8644 resulted in a significant rise of calcium between 17 and 57 mmHg.

Dynamic calcium-constriction relations during vasomotion

BayK 8644 and TEA induced clear calcium spikes and rhythmic constrictions at all pressure levels (Fig. 2). Individual spikes consisted of rapid upstrokes, followed by approximately exponential decays. In many cases multiple spikes were superimposed (Fig. 2C–D). Up to five superimposed spikes were

observed. Single and multiple spikes were often interchanged in irregular sequences. Also, interval between spikes was variable and periods without oscillations occurred. The amplitude of single calcium spikes increased slightly though significantly with pressure. The calcium decay time did not significantly depend on pressure (Fig. 3).

Calcium spikes were associated with vasomotion cycles. However, the diameter could not instantaneously follow the calcium transient and consequently a clear lag was present between peak calcium and peak constriction. These dynamics are analyzed below. When multiple spiking occurred, the diameter response was either a double constriction if sufficient time lag was present between the spikes (Fig. 2B and C third spike) or a single deep constriction when the spikes occurred rapidly after one another (Fig. 2C first two spikes, 2D).

Figure 4A–C shows an example of fitting calcium-diameter relations based on the first-order model I and second order model II to a 30 sec. period of oscillations. Figure 4C depicts the measured calcium signal. Figure 4A indicates the measured diameter signal as well as the prediction by first-order dynamics, while Fig. 4B shows the fit to the second order model. Both latter panels also indicate the deviation between measured and predicted diameter. As can be seen, the fit to model I deviated substantially (r^2 = 0.830) and systematically from the signal, while the error was far less for the second order model II (r^2 = 0.962). The two fits were used to predict the response to a (hypothetic) calcium Dirac impulse (Fig. 4D–F). Such impulse responses characterize the properties of the calcium signalling and contractile machinery in the time domain. The first-order response (Fig. 4D) is by definition an immediate constriction followed by an exponential relaxation. For the second-order fit (Fig. 4E), a finite time elapses before peak constriction is reached. We fitted models I and II to 486 periods of around 30 sec vasomotion. Median r^2 was 0.877 (quartiles 0.720–0.923) for model I, and 0.960 (quartiles 0.891–0.982) for model II. Considering the far tighter fit and less appearance of systematic deviations in model II, below the dynamic properties are only analyzed based on model II.

The effect of pressure on the dynamic calcium-constriction relation was analyzed based on the impulse responses of the fitted second-order models. Figure 5 shows examples of impulse responses for a single vessel at the three pressure levels, together with three descriptive parameters of these responses. Figure 6 summarizes these parameters as functions of the pressure. While the amplitude of the diameter response to the calcium impulse was a clear and significant function of the distending pressure, the effect of pressure on the other impulse response parameters was limited: the time-to-peak and relaxation time in the impulse response were somewhat, though statistically significant, larger at 57 mmHg in comparison to 17 mmHg.

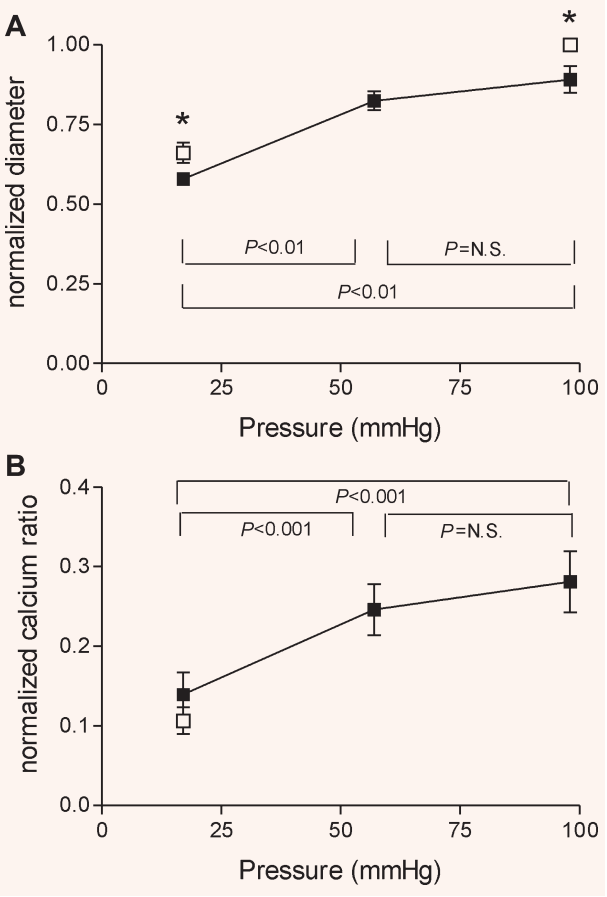

Fig. 1 Time-averaged diameter (**A**) and intracellular calcium, determined from the fura ratio (**B**), as function of the distending pressure. Closed squares: during active tone and vasomotion induced by TEA and BayK8644. Open squares: under fully dilated conditions. **P*<0.05, dilated versus active tone (paired t-tests). Statistics between pressure levels are repeated measures ANOVA and Bonferroni *post-hoc* tests. Error bars are SEM, *n* = 9 vessels.

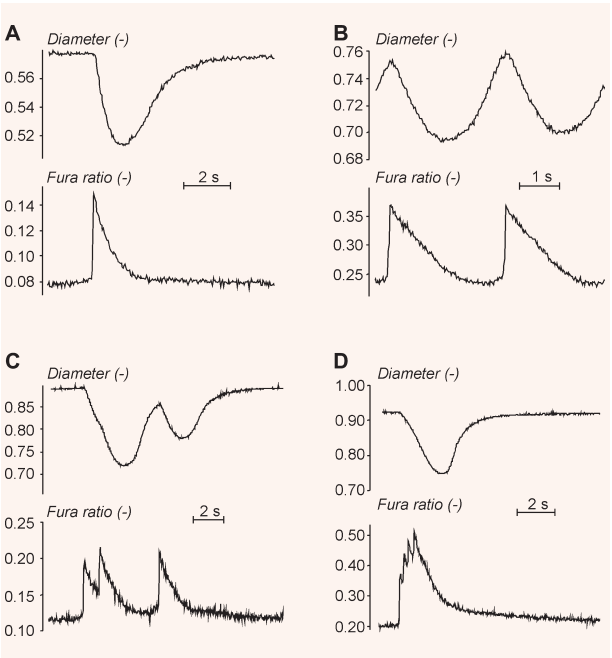

Fig. 2 Examples of simultaneously recorded diameter and calcium oscillations.

Non-isobaric loading

Figure 7 depicts an example of vasomotion during non-isobaric loading. The feedback system was activated for only a few cycles, in order to prevent possible alterations in the level of vasoconstriction. Feedback was always started when the vasomoting vessel was at its maximal diameter. This way, constrictions are exchanged for transient increases in pressure. In this example, three periods of proportional feedback application at increasing gain are shown. As expected, a larger feedback gain resulted in a smaller diameter amplitude and a larger pressure amplitude. Non-isobaric loading for the indicated short periods did not affect the calcium spikes.

Figure 8 plots diameter and pressure amplitudes during non-isobaric loading. The data on the diameter axes reflect isobaric vasomotion (no feedback) at the given baseline pressures, while data points closer to the upper ends of the regression line were obtained during higher feedback gains. The slopes of these lines, in analogy to cardiac muscle, reflect elastance of the activated SMC. Extrapolated intercepts with the pressure axis reflect the amplitude of pressure oscillations during completely isometric loading. These pressure oscillations are proportional to isometric active tension development and thus indicate contractile activation (see discussion). The data in Figure 8 are from four vessels, where episodes with single, double and triple spikes, where available, are separately analyzed. This way, 5–7 curves were obtained for each pressure. For a given baseline pressure, the slopes of the regression lines were similar for single and multiple spiking. For the three baseline pressures, these slopes averaged 3.95±1.77 (n = 5), 6.48±2.45 (n = 7) and 21.4±8.7 (n = 6) mmHg / % diameter change at respectively 17, 57 and 98 mmHg (P<0.001, 98 *versus* 17 and 57 mmHg). For the three experiments with single calcium spikes, the extrapolated intercept with the pressure axis (reflecting true isometric loading) averaged 38, 47 and 44 mmHg at respectively 17, 57 and 98 mmHg basal pressure. The experiments with double spikes had extrapolated isometric pressure oscillations averaging 67 (n = 1), 61 (n = 3) and 66 (n = 2) mmHg at the three basal pressure levels. The intercept was significantly higher for multiple spikes (P<0.01, 1 *versus* 2 and 3 spikes, GLM), but did not depend on the baseline pressure (P = NS).

The dynamics of the calcium effect on diameter may be located in either or both the signalling processes and the smooth muscle cell shortening. If the signalling process were considerably faster than the SMC shortening, then for equal calcium spikes the 'active pressure' transient under isometric loading would be faster than the isobaric diameter transient. Figure 9 plots an example of superimposed calcium spikes and the associated diameter and pressure transients during various degrees of feedback in a single experiment. Increasing the feedback gain resulted in faster diameter transients. Thus, isobaric peak constriction occurred 1.7 sec after start of the calcium transient, while during the highest gain in this example (k = –9.45 mmHg / % diameter change), peak activation occurred after 1.3 sec.

In order to present meaningful averages of peak activation times during non-isobaric loading despite the variable calcium waveforms between the experiments, we again fitted the second-order model and derived impulse response characteristics. This was done only for basal pressures of 17 and 57 mmHg, since at 98 mmHg during feedback the amplitude of the diameter signal was very low, resulting in a poor

signal to noise ratio. Figure 10 plots the amplitude, peak time and relaxation time for both baseline pressures as a function of the feedback gain ($n = 4$). As expected, diameter amplitude of the impulse response (Fig. 10A–D) decreased strongly for higher feedback gains. At the lower pressure, both the peak time and relaxation time decreased slightly with more isometric loading (Fig. 10B–C), while at 57 mmHg baseline pressure, the initial peak time and relaxation times were higher, and the reduction with more isometric loading was larger (Fig. 10E–F). The reductions of not only amplitude, but also peak time and relaxation time at higher feedback gain were significant, both at 17 and 57 mmHg (GLM using dependence on experiment and linear regression with gain, $P<0.005$ for all tests). Thus, the impulse response became shorter at more isometric loading.

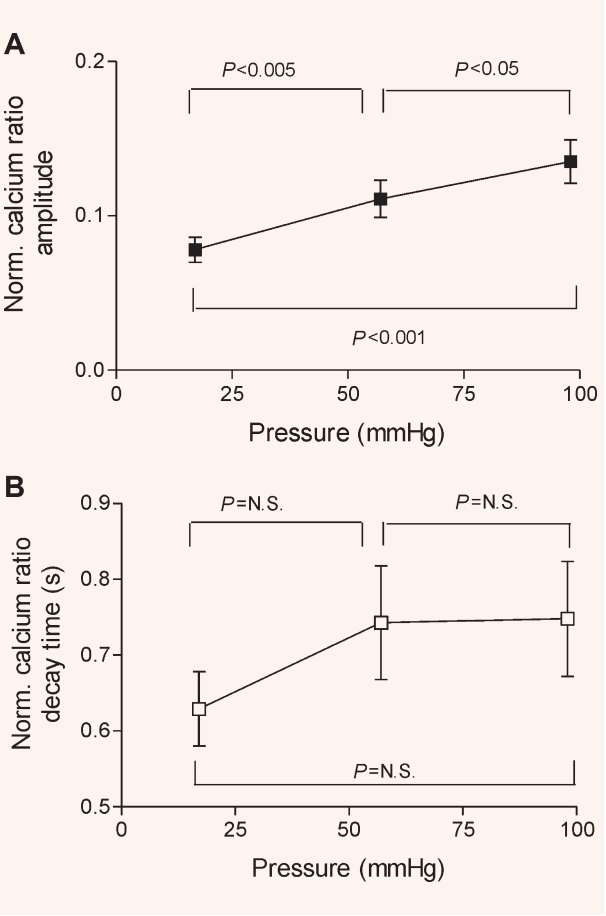

Fig. 3 Characteristics of calcium oscillations: amplitude (**A**) and decay time to half-maximal reduction in the calcium signal (**B**) are shown for cases limited to clear single spikes, such as in Fig. 2A and B. Per vessel, several such spikes were analyzed. Results are mean±SEM of variation between vessels, $n = 7–9$ vessels. Statistics are repeated measures ANOVA and Bonferroni *post-hoc* tests.

Discussion

The purpose of this study was to quantitate the dynamic relation between oscillations in intracellular calcium and the resulting constrictions during drug-induced vasomotion in cannulated rat mesenteric small arteries. There are two main results: firstly, linear second-order dynamics are sufficient to describe this relation. The impulse response of this second-order system had an amplitude that rapidly diminished with increasing pressure levels, while the shape of this response depended in a biphasic way on the pressure, constriction and relaxation being slowest at the intermediate pressure. Secondly, when counteracting diameter excursions during feedback control of the pressure, the impulse responses became faster, indicating that part of the dynamics is related to actual constriction of the vessel. Yet, at the highest applied feedback gains the response to a calcium impulse still lasted ~0.5 sec to peak activation and subsequently ~1 sec to half-maximal relaxation, for both 17 and 57 mmHg baseline pressure. We conclude that these dynamics relate to intracellular signalling.

Rhythmic vasomotion

In order to determine the dynamic calcium-diameter relation, rapid changes in intracellular calcium are needed. We used the ability of mesenteric vessels to develop automacity in calcium and diameter under appropriate conditions. In initial experiments, we found that either the L-type voltage operated calcium channel opener BayK8644 or a calcium-dependent potassium channel blocker alone (TEA or charybdotoxin) resulted in sparse periods of vasomotion. Their combination nearly always induced vasomotion at all pressure levels. Moreover, the calcium oscillations consisted of single or multiple rapid upstrokes, providing sufficient high-frequency information for fitting the calcium-diameter transfer

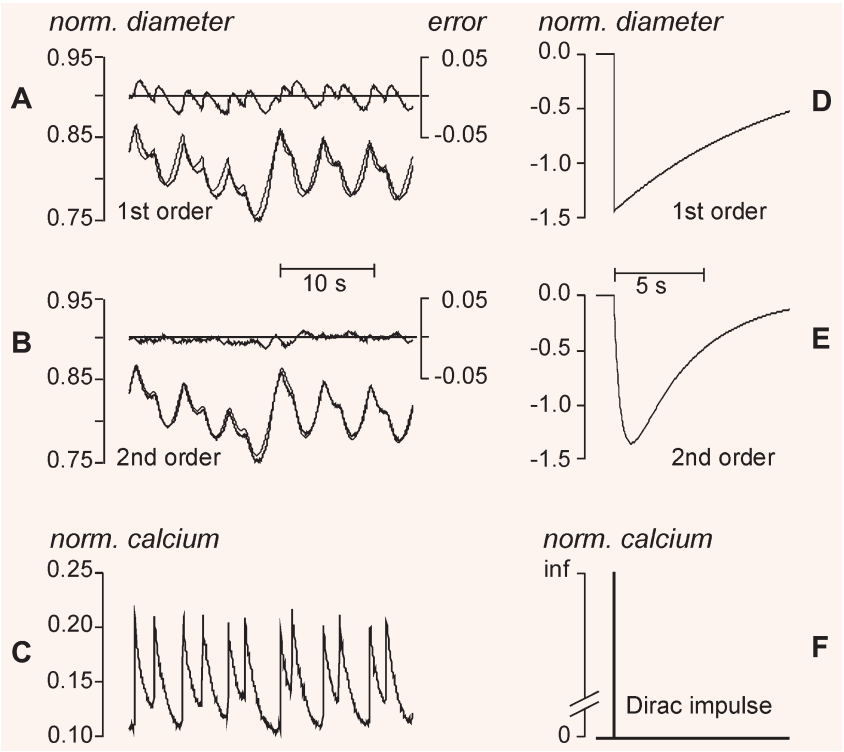

Fig. 4 Illustration of the procedure for fitting linear first-order (**A**) and second-order (**B**) models (thinner lines) to the diameter response (thicker line) following the calcium signal (**C**). Inserts in (**A**) and (**B**) (right axes) denote the deviation between measurement and prediction. (**D**) and (**E**) depict the predicted diameter response for these first and second-order models to a hypothetic dirac pulse (**F**) in the calcium signal.

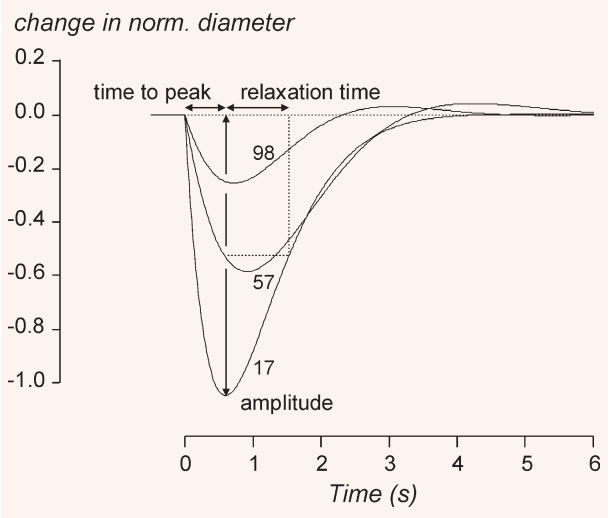

Fig. 5 Example of predicting the diameter response to a hypothetical dirac pulse in the calcium signal for a single vessel at the three studied levels of pressure, using the second-order model. The shape of these curves was characterized by three pragmatic parameters: the time to peak, amplitude and half-maximal diameter relaxation time, shown here for the response at 17 mmHg.

functions. The calcium and diameter signals were determined over several hundred micrometers of vessel length, and the rapid upstroke of the measured calcium spike therefore indicates synchronicity over this length of vessel. We speculate that fluctuations in membrane potential, possibly action potentials, form the base for the calcium spikes. Indeed, the combination of TEA and BayK8644 is expected to destabilize the membrane potential. However, a role for ryanodine receptors in BayK8644-induced vasomotion has been reported for renal afferent arterioles [14]. Whether the current stimulus activates a pure membrane oscillator or whether calcium release is also involved in this model therefore remains to be established. Multiple spikes such as in Fig. 2D could result from either trains of depolarizations or the presence of populations of SMC firing with delays.

Rhythmicity in arterial smooth muscle has recently been reviewed [9, 11] and modelled [15, 16]. In rat mesenteric vessels, rhythmicity is seen spontaneously [10], after application of the calcium channel opener BayK8644 [17, 18], and after stimulation with alpha-adrenergic agonists [10, 19, 20]. In the latter case, the rhythmicity was found to depend on

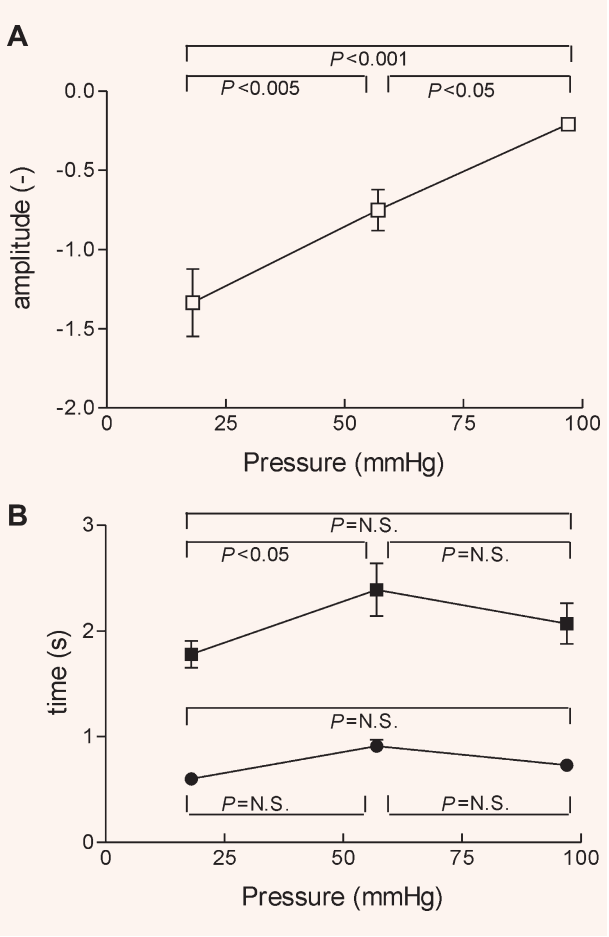

Fig. 6 Average data for the dirac pulse-response parameters amplitude (**A**), time to peak (**B**, circles) and relaxation time (**B**, squares), as function of the pressure. Results are mean±SEM of variation between vessels, $n = 8–9$ vessels. Statistics are repeated measures ANOVA and Bonferroni *post-hoc* tests.

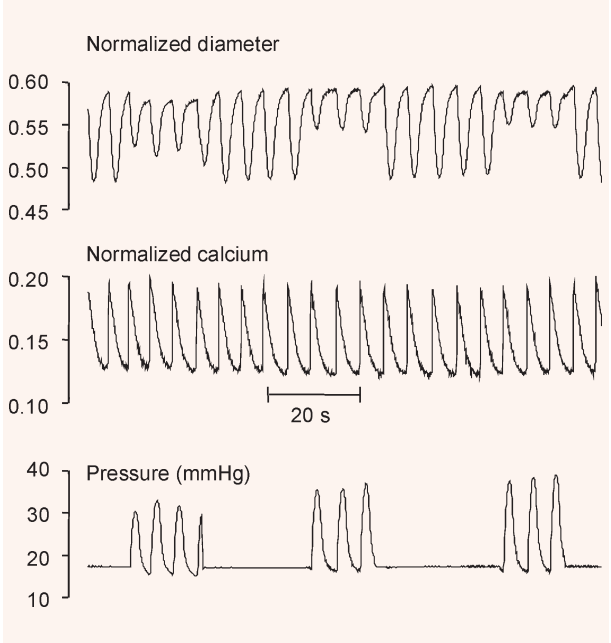

Fig. 7 Example of vasomotion and calcium oscillations during periods of proportional feedback counteracting the constriction by simultaneously raising the pressure. In this particular case, vasomotion was regular. Three periods of increasing feedback gain are shown, leading to smaller diameter excursions and larger pressure oscillations. The calcium signal was not affected by such periods of non-isobaric loading.

synchronization of calcium waves, *via* activation of calcium-dependent chloride channels and oscillations in membrane potential [21]. Conflicting data exist on the role of the endothelium in such synchronization. Sell *et al*. [22] found acetylcholine to desynchronize the calcium oscillations in SMC. Rahman *et al*. on the other hand found that synchronization depends on endothelial nitric oxide, and in denuded vessels can partly be restored by cGMP derivatives [19]. Others have suggested that endothelium-derived hyperpolarizing factors rather than nitric oxide are involved in adrenergic vasomotion in rat mesenteric vessels [23]. A theoretical analysis of vasomotion provides a possible answer to these conflicting findings on the basis of steady and oscillatory domains of intracellular calcium levels [15]. We can also not rule out the possibility that Cajal-like cells, known to be present in not only the intestinal tract but also other visceral organs [24] and blood vessels [25] generated the rhythmicity in the current experiments.

Vasomotion characteristics are well known to depend on the distending pressure, and one might argue that vasomotion is indeed mediated by mechanosensors, such that during the relaxation phase, wall tension increases according to the Laplace law, followed by stimulation of the mechanosensors and a new contraction response. Yet we saw no effect of increasingly isometric loading on calcium spiking. Since excursions in wall stress following activation are opposite under isobaric and isometric conditions [26], this indicates that

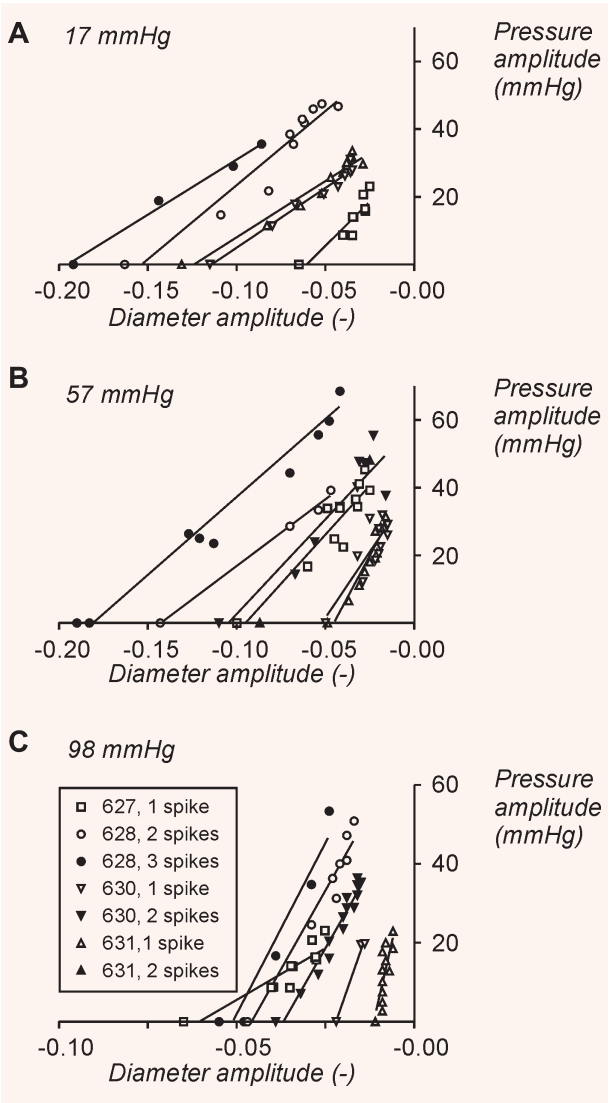

Fig. 8 Load line analysis of vasomotion. Data were separately analyzed for selected periods of regular calcium oscillations with 1–3 spikes in each oscillation. During such oscillations, various degrees of feedback were applied, as was shown by the example of Figure 7. Points on the horizontal axis denote isobaric vasomotion, points closer to the vertical axis indicate more isometric vasomotion. For each feedback level, diameter and pressure amplitude were determined, and their relation was determined by linear regression over the various feedback levels. Symbols are defined in panel C, the numbers are vessel numbers.

mechanosensors do not form part of the feedback loop maintaining rhythmicity, even though they may well modulate the rhythmicity.

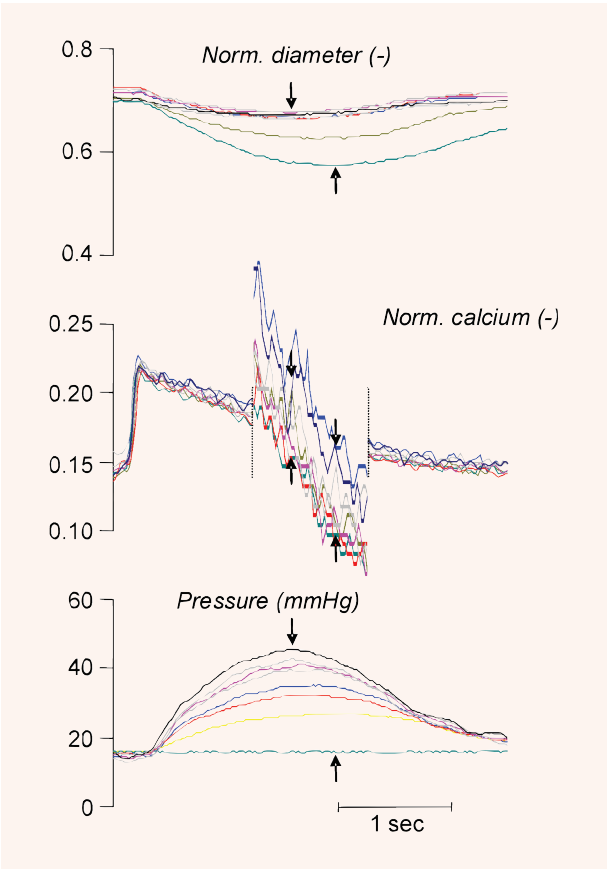

Fig. 9 example of superimposed recordings of normalized diameter, calcium and pressure for isobaric loading and seven levels of increasing feedback. Up and down arrows indicate the time of respectively deepest isobaric constriction level and highest pressure during feedback, and the associated signals (mint and black in colour plot). Middle part of the calcium signals has been vertically stretched to better indicate the individual signals. Note that in the presence of feedback, the peak response occurred earlier, while in this particular case the calcium signal decayed actually somewhat slower.

Calcium sensitivity during vasomotion

A concern of the current study is that myogenic responsiveness was absent under the chosen experimental conditions. Myogenic responses to increasing pressure in these vessels are reported for a variety of conditions, and are caused by a combination of increases in calcium and sensitization [27]. Indeed we previously observed that myogenic responses are potentiated by the L-type calcium opener

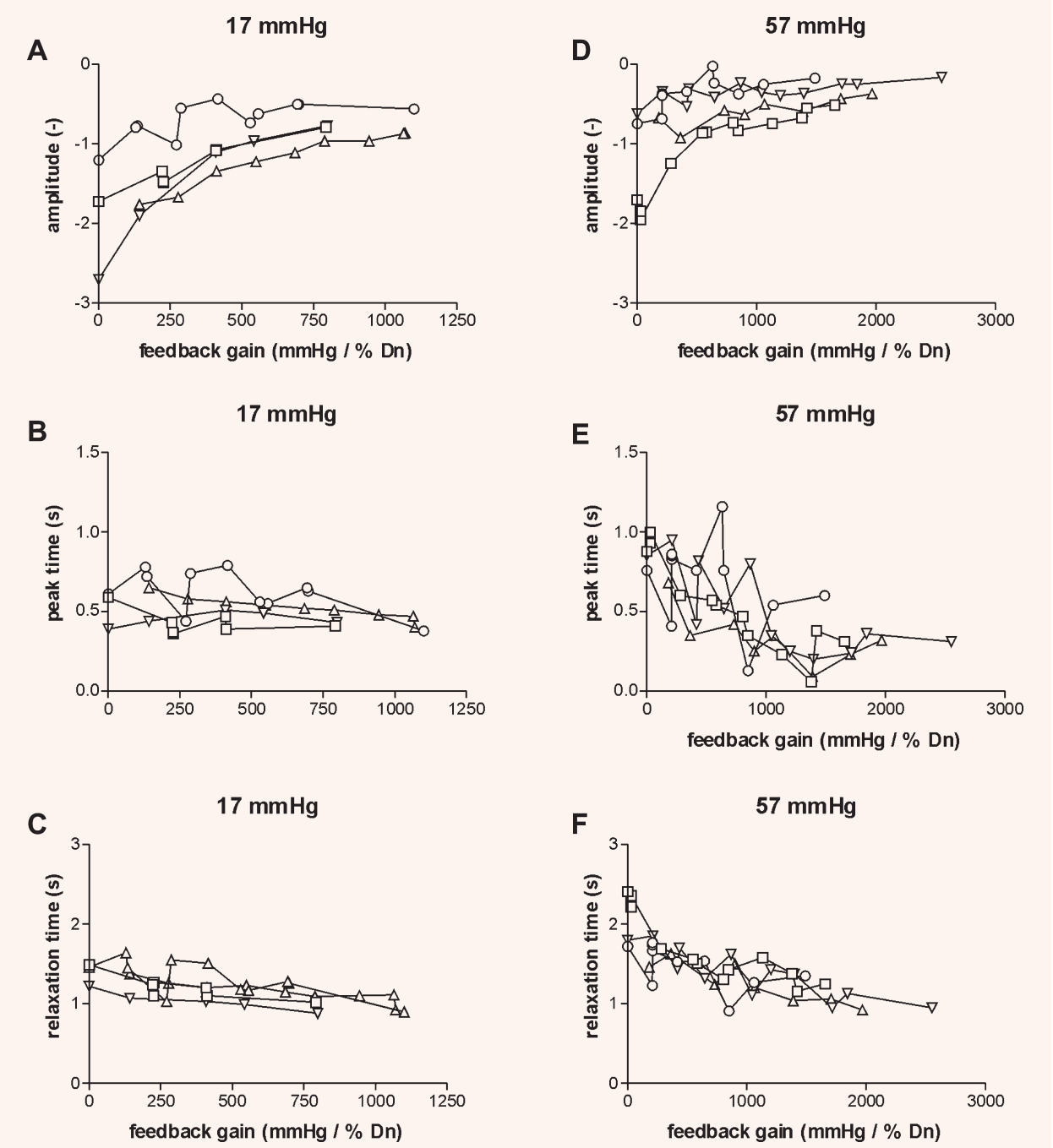

Fig. 10 Dirac pulse parameters for the second-order model (see Fig. 5) during proportional feedback, for a baseline pressure of 17 mmHg (**A**–**C**) and 57 mmHg (**D**–**F**). Individual symbols are separate experiments.

BayK8644 and inhibited by blockers of these channels [28], while simultaneously the calcium-tone relation for pressure is much steeper than for potassium as stimulus, indicating sensitization [3]. Yet, in the current study myogenic responses were absent in the combined presence of BayK8644 and TEA:

vessels did not counteract the distension at higher pressure (Fig. 1A) despite the rise in intracellular calcium (Fig. 1B). A similar suppression of myogenic responsiveness by blocking K_{Ca} channels was found by Wesselman *et al.*, using charybdotoxin during myogenic responsiveness in the presence of noradrenaline [29]. The lack of myogenic responsiveness is attributable to a lack of pressure-induced calcium sensitization under these conditions. The possible causes for this include the continuous presence of calcium spikes. It should thus be remarked that the current dynamic relations hold only for these specific conditions. It remains to be established how the normal pressure-induced calcium sensitization affects these dynamics.

Despite the low-calcium sensitivity, the spikes were sufficient to cause substantial constrictions at all pressures. While amplitudes of constriction were much lower at higher pressure, the feedback experiments reveal similar transients in activation at the three pressures, around ~42 and ~65 mmHg extrapolated peak isometric pressures during respectively single and double spiking (Fig. 8), again indicating a lack of pressure-induced calcium sensitization under these conditions. These pressure excursions are substantial (respectively, ~25% and ~40%) when compared to the maximal level of 160–180 mmHg isometric active pressure development in these vessels [3]. However, the amplitudes in normalized fura ratio were limited. Indeed, the calcium-activation slope during the current vasomotion is steeper than the previously found static one during electromechanical coupling. Thus, even though the vessels were not very sensitive to baseline calcium levels, their sensitivity to calcium spikes was high compared to static elevations in calcium.

Activation and vasoconstriction following calcium transients

Relating the diameter oscillations to SMC activation is complicated due to the Hill force–velocity relationship that is fundamental to muscle activity. Figure 11 shows schematic Hill force–velocity relations for two levels of activation, as well as possible paths of transition when calcium changes. When signalling between calcium and activation is very fast, a calcium step would immediately induce a high constriction velocity, and subsequent dynamics are dominated by the upper Hill curve (transition 1). The subsequent vasoconstriction will then gradually slow because of the decreasing difference between actual load on the contractile elements and isometric tension. Finally, the vessel reaches a new equilibrium. In this case, the diameter response to a calcium step would resemble first-order kinetics. In the second possible case (transition 2), signalling downstream of the calcium rise is a slow process. In this case, the vessel would remain close to mechanical equilibrium during the slowly developing activity, and thus move to the new isometric tension point along the tension axis. Transition 3 is intermediate: after a calcium step, some signalling time is needed before peak constriction velocity is reached.

The current calcium-diameter relations could not be fitted by first-order kinetics (see Fig. 4). This argues against the first case, where signalling is fast. Non-linear first-order models also do not fit the data, because peak constriction velocity clearly lagged peak calcium. The second-order kinetics could also not be fully attributed to the signalling pathway (case 3), since the constriction velocities were clearly dependent on the pressure level, that is, on the load imposed on the vessel. Moreover, the non-isobaric experiments, where diameter excursions were counteracted by pressure variation, show faster dynamics at higher feedback gains. This indicates that part of the dynamics is located in the actual vasoconstriction. Thus, we suggest that the second-order calcium-diameter relation observed in the current study is the result of dynamics present in both the signalling processes and the force-velocity relation (transition 3 in Fig. 11), and estimate that the activation response to a hypothetic calcium impulse takes ~0.5 sec to peak activation and subsequently ~1 sec to half-maximal relaxation.

It could be argued that still higher order models would provide even better fits of these dynamic data. However, we found no systematic deviations for the second-order model (Fig. 4), leaving little reason to apply third-order or non-linear second-order models.

Comparison of current dynamics to other vascular studies

Zimmermann *et al.* [30] analyzed dynamics of the signalling processes from the force transient after photolysis of caged calcium in rabbit portal vein

strips at room temperature. Such a photolysis results in stepwise calcium transients to micromolar levels. Their delay between rise in calcium and onset of force (td) varied from 0.47 sec in the absence of added calmodulin (CaM) to 0.20 sec at 40 μM CaM, indicating that recruitment of CaM is one of the causes of this delay. The delay was followed by a 7.4 (0 μM CaM) to 3.9 sec (40 μM CaM) period before half-maximal tension was reached (t1/2). The kinetics of both force development and myosin light chain (MLC) phosphorylation were much faster after photolysis of caged ATP in the presence of the Ca^{++}-CaM-MLCK complex (td = 50 msec for force), indicating that MLC phosphorylation is hardly a rate-limiting step, and the authors suggest that conformational changes of the latter complex after binding of Ca^{++}-CaM to MLCK account for most of the remaining delay. In the current experiments calcium transients were not stepwise. However, the fitted calcium-diameter relations allowed the prediction of the diameter response to a calcium step: our td's would have been 0.18 ± 0.01, 0.28 ± 0.02 and 0.23 ± 0.02 at respectively 17, 58 and 96 mmHg, and correspond with those of Zimmermann *et al*. in the presence of high CaM levels. Our predicted t1/2 values are faster: 1.13 ± 0.09 sec, 1.42 ± 0.13 sec, and 1.31 ± 0.13 sec at the 3 pressure levels, despite the inclusion of the limited constriction velocity. There are many differences between both studies, including the temperature (37°C in the current study). It is therefore not clear whether the current calcium-diameter dynamics also mainly involve CaM recruitment and conformational changes of the Ca^{++}-CaM-MLCK complex. However, the current model can be used to address such issues in future work.

Few other studies address dynamic calcium-constriction relations in blood vessels. Very recently, Brekke *et al*. [12] studied this relation *in vivo* in hamster cheek pouch arterioles. Spontaneous vasomotion, when occurring, was associated with a rapid upstroke in calcium, after ~2 sec followed by onset of vasoconstriction. Vasoconstriction then continued until the calcium level suddenly fell again. Upon stepwise application of phenylephrine for 1 sec, a ~1 sec delay in onset between calcium and vasoconstriction was found, while delay between peak calcium and peak constriction was ~5 sec. Despite the many differences with the current study, including species, tissue, size of vessels, stimulus, and *in vivo* versus *in vitro* settings, the dynamics are reasonably comparable.

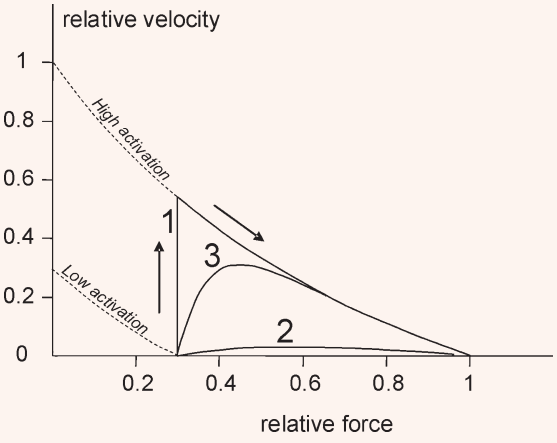

Fig. 11 Schematic force-velocity relation for a vessel undergoing a transition from low to high activation. The dashed lines indicate the Hill curves for two levels of activation. Three possible transitions from a low-activation to a high-activation steady state are shown: transition **1** reflects the case where the low constriction velocity of smooth muscle dominates the dynamics, **2** indicates the case where dynamics are dominated by intracellular signalling, and **3** is intermediate.

Analogy to contracting myocardium

The regression lines in Fig. 8 bear some analogy with left ventricular end-systolic pressure–volume curves: by varying the degree of isometric feedback, the vessels were allowed to reduce volume at a constant 'preload', or to build up an active, 'systolic', pressure. In the heart, stroke volume and peak isovolumetric pressure increase strongly with preload. This was not the case in the current vessels: extrapolated isometric peak active pressure was identical when tested at preloads between 17 and 98 mmHg: ~42 and ~65 mmHg above the preload for respectively single and double calcium spikes. Diameter amplitudes (resembling stroke volume) at the various degrees of isometric feedback were clearly lower at higher baseline pressures. Thus, our vessels lacked a Frank-Starling mechanism. The causes for this may possibly include geometric differences, the slow contraction velocity, the high elastic forces, and the relatively flat active length–tension curve [3] in the tested diameter range.

Conclusion

In conclusion, we used vasomoting blood vessels to determine the dynamics between calcium spiking, activation and constriction. While this work has not addressed specific molecular mechanisms and may therefore seem rather descriptive, we do believe that we provide a new approach that in future work can add to the unravelling of signalling cascades associated with contractile activation in small arteries. In particular, the use of specific blockers or genetic models generally induces up-regulation of compensatory pathways. Static calcium-constriction relations may therefore be relative unaffected, but slowing down of dynamic relations after intervention would be clear evidence that critical pathways are blocked. Applying this dynamic approach would thus allow further unravelling of mechanisms of vascular diameter control in health and disease.

Reference

1. **Karaki H.** Ca^{2+} localization and sensitivity in vascular smooth muscle. *Trends Pharmacol Sci.* 1989; 10: 320–5.
2. **Ratz PH, Berg KM, Urban NH, Miner AS.** Regulation of smooth muscle calcium sensitivity: KCl as a calcium-sensitizing stimulus. *Am J Physiol Cell Physiol.* 2005; 288: C769–83.
3. **VanBavel E, Wesselman JP, Spaan JA.** Myogenic activation and calcium sensitivity of cannulated rat mesenteric small arteries. *Circ Res.* 1998; 82: 210–20.
4. **Uehata M, Ishizaki T, Satoh H, Ono T, Kawahara T, Morishita T, Tamakawa H, Yamagami K, Inui J, Maekawa M, Narumiya S.** Calcium sensitization of smooth muscle mediated by a Rho-associated protein kinase in hypertension. *Nature.* 1997; 389: 990–4.
5. **Budzyn K, Marley PD, Sobey CG.** Targeting Rho and Rho-kinase in the treatment of cardiovascular disease. *Trends Pharmacol Sci.* 2006; 27: 97–104.
6. **VanBavel E, Van der Meulen ET, Spaan JA.** Role of Rho-associated protein kinase in tone and calcium sensitivity of cannulated rat mesenteric small arteries. *Exp Physiol.* 2001; 86: 585–92.
7. **Carvajal JA, Germain AM, Huidobro-Toro JP, Weiner CP.** Molecular mechanism of cGMP-mediated smooth muscle relaxation. *J Cell Physiol.* 2000; 184: 409–20.
8. **Yang J, Clark JW, Bryan RM, Robertson CS.** Mathematical modeling of the nitric oxide/cGMP pathway in the vascular smooth muscle cell. *Am J Physiol Heart Circ Physiol.* 2005; 289: H886–97.
9. **Haddock RE, Hill CE.** Rhythmicity in arterial smooth muscle. *J Physiol.* 2005; 566: 645–56.
10. **VanBavel E, Giezeman MJ, Mooij T, Spaan JA.** Influence of pressure alterations on tone and vasomotion of isolated mesenteric small arteries of the rat. *J Physiol.* 1991; 436: 371–83.
11. **Aalkjaer C, Nilsson H.** Vasomotion: cellular background for the oscillator and for the synchronization of smooth muscle cells. *Br J Pharmacol.* 2005; 144: 605–16.
12. **Brekke JF, Jackson WF, Segal SS.** Arteriolar smooth muscle Ca^{2+} dynamics during blood flow control in hamster cheek pouch. *J Appl Physiol.* 2006; 101: 307–15.
13. **VanBavel E, Mooij T, Giezeman MJ, Spaan JA.** Cannulation and continuous cross-sectional area measurement of small blood vessels. *J Pharmacol Methods.* 1990; 24: 219–27.
14. **Takenaka T, Ohno Y, Hayashi K, Saruta T, Suzuki H.** Governance of arteriolar oscillation by ryanodine receptors. *Am J Physiol Regul Integr Comp Physiol.* 2003; 285: R125–31.
15. **Koenigsberger M, Sauser R, Beny JL, Meister JJ.** Role of the endothelium on arterial vasomotion. *Biophys J.* 2005; 88: 3845–54.
16. **Koenigsberger M, Sauser R, Lamboley M, Beny JL, Meister JJ.** Ca^{2+} dynamics in a population of smooth muscle cells: modeling the recruitment and synchronization. *Biophys J.* 2004; 87: 92–104.
17. **Hill MA, Meininger GA.** Calcium entry and myogenic phenomena in skeletal muscle arterioles. *Am J Physiol.* 1994; 267: H1085–92.
18. **Achakri H, Stergiopulos N, Hoogerwerf N, Hayoz D, Brunner HR, Meister JJ.** Intraluminal pressure modulates the magnitude and the frequency of induced vasomotion in rat arteries. *J Vasc Res.* 1995; 32: 237–46.
19. **Rahman A, Matchkov V, Nilsson H, Aalkjaer C.** Effects of cGMP on coordination of vascular smooth muscle cells of rat mesenteric small arteries. *J Vasc Res.* 2005; 42: 301–11.
20. **Shaw L, O'Neill S, Jones CJ, Austin C, Taggart MJ.** Comparison of U46619-, endothelin-1- or phenylephrine-induced changes in cellular Ca^{2+} profiles and Ca^{2+} sensitisation of constriction of pressurised rat resistance arteries. *Br J Pharmacol.* 2004; 141: 678–88.
21. **Peng H, Matchkov V, Ivarsen A, Aalkjaer C, Nilsson H.** Hypothesis for the initiation of vasomotion. *Circ Res.* 2001; 88: 810–5.

22. **Sell M, Boldt W, Markwardt F.** Desynchronising effect of the endothelium on intracellular Ca^{2+} concentration dynamics in vascular smooth muscle cells of rat mesenteric arteries. *Cell Calcium.* 2002; 32: 105–20.
23. **Mauban JR, Wier WG.** Essential role of EDHF in the initiation and maintenance of adrenergic vasomotion in rat mesenteric arteries. *Am J Physiol Heart Circ Physiol.* 2004; 287: H608–16.
24. **Popescu LM, Ciontea SM, Cretoiu D.** Interstitial Cajal-like cells in human uterus and fallopian tube. *Ann N Y Acad Sci.* 2007; 1101: 139–65.
25. **Harhun MI, Pucovsky V, Povstyan OV, Gordienko DV, Bolton TB.** Interstitial cells in the vasculature. *J Cell Mol Med.* 2005; 9: 232–43.
26. **VanBavel E, Mulvany MJ.** Role of wall tension in the vasoconstrictor response of cannulated rat mesenteric small arteries. *J Physiol.* 1994; 477: 103–15.
27. **Davis MJ, Hill MA.** Signaling mechanisms underlying the vascular myogenic response. *Physiol Rev.* 1999; 79: 387–423.
28. **Wesselman JP, VanBavel E, Pfaffendorf M, Spaan JA.** Voltage-operated calcium channels are essential for the myogenic responsiveness of cannulated rat mesenteric small arteries. *J Vasc Res.* 1996; 33: 32–41.
29. **Wesselman JP, Schubert R, VanBavel ED, Nilsson H, Mulvany MJ.** KCa-channel blockade prevents sustained pressure-induced depolarization in rat mesenteric small arteries. *Am J Physiol.* 1997; 272: H2241–9.
30. **Zimmermann B, Somlyo AV, Ellis-Davies GC, Kaplan JH, Somlyo AP.** Kinetics of prephosphorylation reactions and myosin light chain phosphorylation in smooth muscle. Flash photolysis studies with caged calcium and caged ATP. *J Biol Chem.* 1995; 270: 23966–74.